Microchimica Acta (2019) 186: 314
https://doi.org/10.1007/s00604-019-3403-z

ORIGINAL PAPER

A fluorometric aptamer nanoprobe for alpha-fetoprotein by exploiting the FRET between 5-carboxyfluorescein and palladium nanoparticles

Guiyin Li[1] · Junxiang Zeng[1] · Huiling Liu[1] · Ping Ding[2] · Jintao Liang[1] · Xinmin Nie[3] · Zhide Zhou[1]

Received: 14 December 2018 / Accepted: 2 April 2019 / Published online: 30 April 2019

Abstract

Alpha-fetoprotein (AFP) is a reliable clinical marker of hepatocellular carcinoma (HCC). A highly sensitive fluorometric aptamer nanoprobe is described for AFP detection. It is based on fluorescence resonance energy transfer (FRET) between AFP aptamer labelled with 5-carboxyfluorescein (FAM) and palladium nanoparticles (PdNPs). The PdNPs quench the green fluorescence of the FAM-AFP aptamer via interactions between nitrogen functional groups of the AFP aptamer and PdNPs. When AFP was introduced into the FAM-AFP aptamer-PdNPs FRET system, the AFP aptamer preferentially combines with AFP. This results in a conformational change and weakens the interaction between the aptamer and the PdNPs. Thus, the fluorescence of FAM recovers. The fluorescence recovery of FAM increases linearly in the 5.0–150 ng·mL^{-1} AFP concentration range and has a 1.4 ng·mL^{-1} detection limit. The assay was applied to the analysis of spiked diluted human serum. The recovery values ranged from 98.3 to 112.9%, with relative standard deviations of <1.1%. This biosensing strategy provides a reliable and ultrasensitive protocol for the quantification of biomarkers with relevant antigens and aptamers.

Keywords Fluorescence resonance energy transfer · Alpha-fetoprotein · Palladium nanoparticles · Aptamer

Introduction

Tumor markers are biological molecules secreted by a tumor or a specific response of the body to the cancer, and have been proved to be associated with carcinogenesis [1]. Alpha-fetoprotein (AFP), a reliable clinical tumor marker of hepatocellular carcinoma (HCC), is a glycoprotein found in the yolk sac and secreted from the fetal liver in early embryonic life, which is later mainly derived from the liver [2]. In the serum of healthy human, the average level of AFP is below 25 ng·mL^{-1}, but it increases obviously to 400 ng·mL^{-1} in nearly 75% HCC patients. An elevated AFP concentration in adult serum is widely considered as an early indication of HCC or endodermal sinus tumor [3, 4]. Therefore, sensitive and accurate AFP detection is of great significance for the early clinical diagnosis, portable medical supervision and long-term treatment.

Various strategies have been explored for the detection AFP, such as enzyme immunoassay [5], lateral flow immunoassay [6], fluorescence immunoassay [7], electrochemical biosensor [8], electrochemiluminescence assay [9] and so on. Among the above assays, fluorescent sensing, especially fluorescence resonance energy transfer (FRET)-based technique, has attracted great attention because of high sensitivity, low cost and simple operation [10]. FRET is a process that

Electronic supplementary material The online version of this article (https://doi.org/10.1007/s00604-019-3403-z) contains supplementary material, which is available to authorized users.

✉ Xinmin Nie
niexinmin7440@sina.com

✉ Zhide Zhou
zzdlgy@163.com

[1] School of Life and Environmental Sciences, Guilin University of Electronic Technology, Guilin 541004, Guangxi, China

[2] Xiang Ya School of Public Health, Central South University, Changsha 410078, Hunan, China

[3] Clinical Laboratory of the Third Xiangya Hospital, Central South University, Changsha 410013, Hunan, China

employs fluorescence particles as donors and quencher particles as acceptors, where the fluorescence of the donor can be quenched by the acceptor when the donor is immediately adjacent to the acceptor [11, 12]. The change of fluorescence intensity before and after quenching is used to monitor the concentrations of targets. Until now, many FRET-based nanoprobes have been developed to accomplish detection of diverse tumor markers [13, 14]. For example, Shenghao Xu et al. [14] had developed an aptamer induced "switch on" FRET-biosensor for the simultaneous detection of AFP and carcinoembryonic antigen (CEA) combining molybdenum disulfide (MoS_2) nanosheets as energy acceptors and multicolored gold nanocluters (Au NCs) as energy donors.

In the FRET-based analysis, the fluorescence quenching ability of energy acceptors plays an important role in determining the analytical sensitivity. A series of nanomaterials including graphene oxide (GO), carbon nanotubes (CNTs), palladium nanoparticles (PdNPs), gold nanoparticles (AuNPs), MoS_2 nanosheet and metalorganic frameworks (MOFs) have been used as energy acceptors to construct FRET based sensing platforms [15–17]. Among them, PdNPs have received great attention as an energy acceptor for FRET-based biological analysis owing to their big surface areas, high loading of receptor molecules and good biocompatibility [16]. Moreover, PdNPs have excellent binding capability with DNA because there was a strong coordination effect between nitrogen functional groups of DNA and PdNPs [18, 19]. Hui Li et al. [18] proposed a simple method for detection of aflatoxin M_1 in milk by using PdNPs as quencher which can quench the fluorescence of 5-carboxyfluorescein (FAM) attached to aptamer of aflatoxin M_1.

Aptamers are single stranded DNA or RNA molecules selected in vitro through systematic evolution of ligand by exponential enrichment (SELEX). Aptamers have a flexible configuration that recognizes and binds to the related target in a specific and high binding affinity via an adaptive recognition manner [20]. Thus, aptamers have gained increasing interest as potential candidates for biomolecular recognition in the diagnostic and therapeutic fields. And the aptamer-based methods are attractive due to their sensitivity, selectivity and low cost [21, 22]. In recent years, several AFP specific aptamers were successfully screened by SELEX strategy and has been introduced into the detection system for AFP detection with good selectivity [23, 24]. Biqing Bao and co-works [25] have developed a simple and label-free fluorescent aptasensor for detection of AFP based on cationic conjugated polyelectrolytes and aptamer with the detection limit of 1.76 $ng \cdot mL^{-1}$. These results indicate that the aptamer-based methods for AFP detection have become a hotspot of research.

An aptamer/PdNPs FRET-based assay for AFP detection is presented. This assay is based on FRET between AFP aptamer labelled with 5-carboxyfluorescein (FAM) and PdNPs. Aptamer bind specific target to form compact and folded structures, thus AFP aptamer is used as recognition elements in this assay. Firstly, FAM-AFP aptamer was adsorbed onto the surface of PdNPs via strong coordination interactions between nitrogen atom of the nucleobase in the AFP aptamer and the Pd atom of the PdNPs. Thus, the fluorescence of the FAM is quenched by PdNPs based on FRET from the FAM-AFP aptamer to the PdNPs. Secondly, upon the addition of AFP markers, green fluorescence will be recovered along with the releasing of FAM-AFP aptamer, because of the higher affinity between aptamer and target. Therefore, a highly sensitive strategy for AFP detection is achieved by the fluorescence change in the absence and presence of AFP. The application of AFP aptamer with high affinity and specificity towards AFP contributed to the good performance of this fluorescence strategy in both aqueous buffer solution and human serum samples.

Experimental

Reagents and materials

Alpha-fetoprotein (AFP), immunoglobulin G (Ig G), immunoglobulin E (Ig E), Bovine serum albumin (BSA) and Human serum albumin (HSA) were obtained from Aladdin Reagents Ltd. (Shanghai, China, http://www.aladdin-e.com/). Ascorbic acid (AA), Sodium tetrachloropalladate (Na_2PdCl_4), palladium dichloride ($PdCl_4$) and sodium citrate ($Na_3C_6H_5O_7$) were supplied by Shanghai Linc-Bio Science Co., Ltd. (Shanghai, China, http://www.linc-bio.com/). An ssDNA aptamer for AFP was employed as the targeting ligand and synthesized by Shanghai Sangon Biotechnology Co., Ltd. (Shanghai, China, https://www.sangon.com/). The sequence of the FAM-AFP aptamer was 5'-FAM-GTGACGCTCCTAACGCTGACTCAGGTGCAGTTCTCGACTCGGTCTTGATGTGGGTCCTGTCCGTCCGAACCAATC-3′ [23]. All reagents were of analytical grade purity and without any further purification. All solutions were prepared with ultrapure water of 18 MΩ·cm resistivity purified from Milli-Q purification system (Milli-Pore, Bedford, MA, USA).

Apparatus

Fluorescence measurements were performed on an F-4600 fluorometer (Hitachi Co. Ltd., Japan, http://www.hitachi.com/). The UV-vis absorption measurements were conducted on a 756CRT spectrophotometer (Shanghai Precision Scientific Instrument Co., Ltd., China, http://www.spsic.com/). The morphologies and surface structures of the PdNPs were observed with scanning electron microscopy (SEM, Quanta 200, Field Electron and Ion Company, USA, https://www.fei.com/), Transmission electron microscopy

(TEM, JEM-2100F, Japan, https://www.jeol.co.jp/) and Malvern Instruments Zeta sizer (Nano-ZS Series, Almelo, Netherlands, https://www.malvernpanalytical.com.cn/).

Preparation of the palladium nanoparticles (PdNPs)

PdNPs were synthesized through a seed-mediated growth method reported by Li et al. with minor modified [18]. In brief, 20% sodium citrate (100 μL) solution and 1% Na_2PdCl_4 aqueous solution (735 μL) were both added into 47.0 mL ultrapure water. After the solution was heated to boiling, 0.1% hot sodium ascorbate solution (2.5 mL) was introduced quickly into the mixture and continued to react for 30 mins under boiling reflux. Then the mixture solution was cooled down to room temperature and filtered through a 0.22 μm millipore membrane filter. Thus, the sodium citrate capped palladium seeds were synthesized.

10 mL 1.0 mmol·L^{-1} H_2PdCl_4 solution and 3.0 mL of the synthesized palladium seeds were added into a 50 mL round-bottom flask. Then 1.2 mL 100.0 mmol·L^{-1} ascorbic acid was introduced into the above solutions and stirred for another 5 mins at room temperature. Next, the mixture was centrifuged for 15 mins (10,000 r·min^{-1}), removed the supernatant and washed three times with ultrapure water. Finally, the PdNPs were obtained after drying in vacuum for 3 h.

Construction of the FRET-based aptamer nanoprobe and detection of AFP

To construct the FRET-based aptamer nanoprobe, 20 μL PdNPs (0.21 mg·mL^{-1}) and 20 μL FAM-AFP aptamer (180.0 nmol·L^{-1}) were added to 300 μL HEPES buffer (20 mmol·L^{-1}, pH 6.5, containing 5.0 mmol·L^{-1} KCl and 5.0 mmol·L^{-1} $MgCl_2$) and the resulting solution was incubated for 60 mins. The fluorescence intensity was recorded under excitation at 480 nm and emission at 520 nm. The time-dependent fluorescence intensities were obtained by incubating a fixed concentration of FAM-AFP aptamer (80.0 nmol·L^{-1}) with PdNPs in a concentration of 0.21 mg·mL^{-1} from 1 min to 80 mins.

Next, the FAM-AFP aptamer-PdNPs ensemble assay in HEPES buffer was employed for the determination of AFP. This FRET-based aptamer nanoprobe exhibited weak fluorescence intensity ($\lambda_{excitation/emission}$ = 480/520 nm) in the absence of AFP (F_0). The fluorescence intensity ($\lambda_{excitation/emission}$ = 480/520 nm) of the nanoprobe was recovered upon addition of various concentrations of AFP (F_1). In a typical FRET analysis process, 20 μL PdNPs (0.21 mg·mL^{-1}) and 20 μL FAM-AFP aptamer (180.0 nmol·L^{-1}) were added to 300 μL HEPES buffer (20 mmol·L^{-1}, pH 6.5, containing 5.0 mmol·L^{-1} KCl and 5.0 mmol·L^{-1} $MgCl_2$) and the resulting solution was incubated for 60 mins. Subsequently, 20.0 μL AFP solution of different concentration was introduced to the above FRET analysis system and incubated for 70 mins at room temperature. Finally, the fluorescence emission spectra of the reaction mixture was collected and the fluorescence intensity was measured underλexcitation/emission = 480/520 nm.

To examine the specificity of the FRET-based aptamer nanoprobe, a list of other protein including BSA, HSA, lgG and lgE were added into the FAM-AFP aptamer-PdNPs FRET system in place of AFP following the same experimental procedures.

Detection AFP in human serum samples

To demonstrate the possible application of the proposed method, human serum samples were assayed using the standard addition method by the FAM-AFP aptamer-PdNPs FRET system. The human serum samples were acquired from 181st Hospital of Chinese People's Liberation Army (Guilin, China). The level of AFP in the human serum samples was first detected using the clinical chemiluminescence immunoassay method in the Inspection Center of the 181st Hospital of Chinese People's Liberation Army.

0.5 mL of human serum were taken and added into HEPES buffer to reach a total volume of 5.0 mL. Then 10.0 μL of diluted human serum and 10.0 μL of different concentration of standard AFP solution (20, 40, 60 ng·mL^{-1}) were mixed to prepare a variety of spiked samples. The level of AFP in the spiked sample was measured in parallel 3 times using the developed FAM-AFP aptamer-PdNPs FRET system.

Results and discussion

Characterization of the palladium nanoparticles

Figure 1a displays the characteristic TEM image of PdNPs. Spherical dots are evident from the TEM image, and the PdNPs are well dispersed with the uniform diameter in the range of 50–70 nm. SEM image of PdNPs (Fig. 1b) reveals that the PdNPs exhibit spherical shape with size ranging between 60 and 80 nm. These bright spheres confirm the crystalline nature of the produced PdNPs.

Furthermore, the diameter (d) and surface charge Zeta potential of PdNPs were measured using a Nano-ZS Zeta Sizer. As shown in Fig. 1c, dynamic light scattering measurements reveal that the average size of the PdNPs is approximately 295 ± 35.5 nm, which was bigger than determined by TEM/SEM, presumably arising from the dry state of the TEM/SEM measurement.

Zeta potential analysis is one of the most important and effective means to characterize the surface charges of biomass materials due to the close relationship between the Zeta potential and adsorb ability. As shown in Fig. 1d, the Zeta potential of PdNPs is −5.71 ± 0.8 mV, which is better to avoid

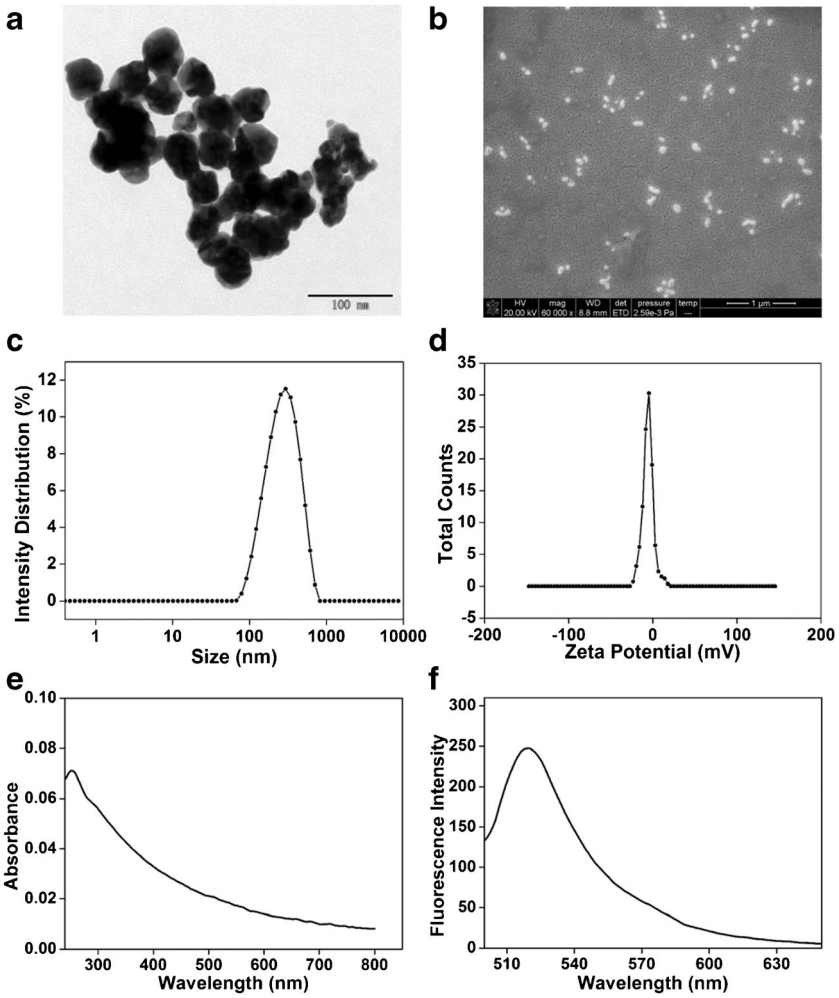

Fig. 1 **a** TEM images of PdNPs; (**b**) SEM images of PdNPs; (**c**) Dynamic light scattering measurements of PdNPs; (**d**) The surface charge Zeta potential of PdNPs; (**e**) Ultraviolet-visible (UV-Vis) absorption spectra of PdNPs; (**f**) The fluorescence emission spectra of FAM-AFP aptamer ($\lambda_{excitation/emission}$ = 480/520 nm)

the side effect caused by electrostatic attraction, because the FAM-AFP aptamer and the PdNPs are all negatively charged [19].

Figure 1e is the UV-vis absorption spectrum of PdNPs, which shows a broad absorption in nearly the whole UV-vis spectral range (from 250 to 600 nm). The absorbance spectrum of PdNPs overlaps well with the fluorescence emission of the FAM-labeled AFP aptamer (Fig. 1f, the maximal emission at 520 nm). So it can be safely inferred that PdNPs has the potential to be effective fluorescence quencher for FAM-labeled AFP aptamer, resulting in the FRET between the FAM-AFP aptamer and PdNPs.

Principle of fluorometric aptamer nanoprobe for AFP

The AFP fluorometric aptamer nanoprobe based on the conformational change of AFP aptamer after interacting with AFP was proposed using FAM as the FRET donor and PdNPs as the FRET acceptor. The principle of the AFP fluorometric aptamer nanoprobe is illustrated in Fig. 2. In the absence of AFP, the FAM-modified AFP aptamer exists in a random coil, and is easily adsorbed on the surface of the PdNPs via strong coordination interactions between nitrogen atom of the nucleobase in the AFP aptamer and the Pd atom of the PdNPs. The strong coordination interactions brought the fluorescence donor FAM close to the fluorescence acceptor PdNPs, which results in the occurrence of FRET, and the fluorescence quenching of FAM is observed. Upon the addition of AFP into the FAM-AFP aptamer-PdNPs FRET system, the FAM-AFP aptamer preferentially binds to AFP, accompanied with its conformational change to form a folded structure, which largely weakens the coordination effect between the AFP aptamer and PdNPs. Thus, the distance between FAM-AFP aptamer and PdNPs is widened and the FRET process was blocked. Therefore the fluorescence of FAM is recovered and the degree of fluorescence recovery is in a positive AFP concentration-dependent manner.

The feasibility of fluorescence AFP detection based on FAM-AFP aptamer and PdNPs

The feasibility of fluorescence AFP detection based on FAM-AFP aptamer and PdNPs was evaluated at different system with HEPES buffer. From Fig. 3a, in the

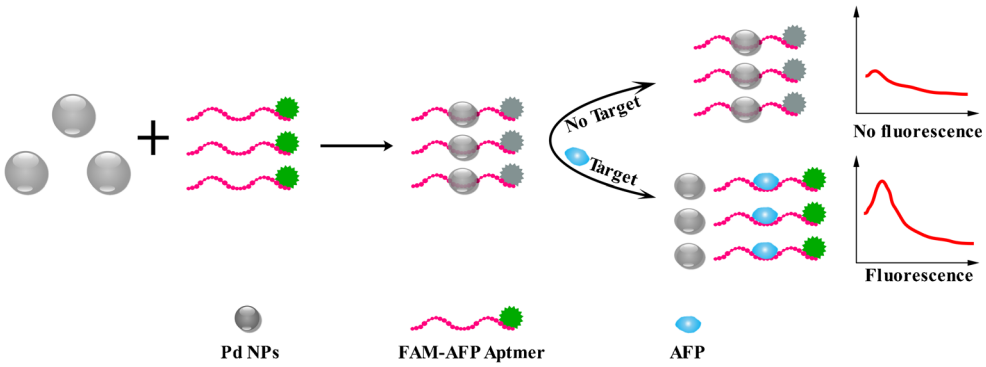

Fig. 2 Schematic illustration of the fluorometric aptamer nanoprobe based on aptamer-bridged FRET from FAM to PdNPs

absence of AFP, the fluorescence intensity of the system (curve a in Fig. 3a) is lower. This was that the fluorescence intensity of FAM-AFP aptamer was quenched through FRET process (FAM-aptamer as donor and PdNPs as acceptor) due to FAM-AFP aptamer absorbed onto the surface of PdNPs via coordination interactions [18]. While in the presence of AFP (2.0 μg·mL^{-1}, curve b in Fig. 3a), the fluorescence of the system is recovered to high intensity. In addition, the fluorescence of the system recovered better with the increasing of AFP concentration (5.0 μg·mL^{-1}, curve c in Fig. 3a). This is the fact that AFP with higher affinity bound FAM-AFP aptamer and their structure change from random conformation to compact and folded structures. Therefore, the FAM-AFP aptamer is not adsorbed by the PdNPs. Hence, it blocks the FRET process and, consequently, the fluorescence of FAM is recovered. The degree of fluorescence recovery is in a positive AFP concentration-dependent

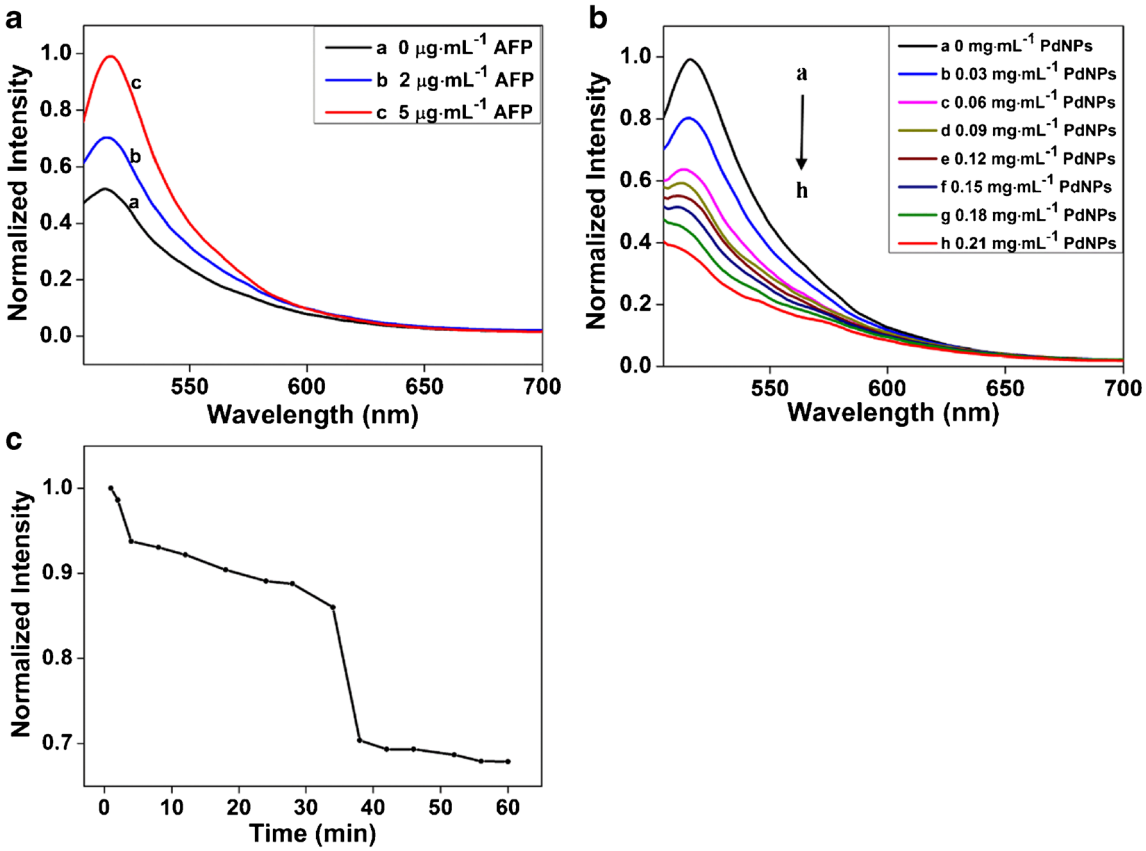

Fig. 3 **a** The feasibility of fluorescence AFP detection based on FAM-AFP aptamer and PdNPs (FAM-AFP aptamer: 180 nmol·L^{-1}; PdNPs: 0.21 mg·mL^{-1}; AFP: 0, 2.0 μg·mL^{-1}, 5.0 μg·mL^{-1}); (**b**) Fluorescence quenching of FAM-aptamer (180 nmol·L^{-1}) after introduction of different concentrations of PdNPs (0, 0.03 mg·mL^{-1}, 0.06 mg·mL^{-1}, 0.09 mg·mL^{-1}, 0.12 mg·mL^{-1}, 0.15 mg·mL^{-1}; 0.18 mg·mL^{-1}; 0.21 mg·mL^{-1}); (**c**) Time dependence of the fluorescence quenching degree for 80 nmol·L^{-1} FAM-labeled AFP aptamer caused by 0.21 mg·mL^{-1} PdNPs. All experiments were performed in HEPES buffer under excitation at 480 nm and emission at 520 nm

manner. Therefore, AFP can be detected sensitively based on the enhanced fluorescent intensity.

Construction of the fluorometric aptamer nanoprobe

To establish a FRET assay with high quenching efficiency, it is important to optimize the ratio between the donor molecules and the quencher molecules. In order to get the optimal ratio between FAM-labeled AFP aptamer and PdNPs for maximum quenching efficiency, 20 μL FAM-AFP aptamer solution (80 nmol·L^{-1}) and 20 μL of a series of concentrations of PdNPs ranging from 0 to 0.21 mg·mL^{-1} were added into 300 μL HEPES buffer, incubated for 60 mins and measured the fluorescence signals. Fig. 3b shows the fluorescence spectra of FAM-aptamer in the presence of different concentrations of PdNPs. It can be seen from Fig. 3b that PdNPs can interact with FAM-AFP aptamer and quench its fluorescence. The maximum fluorescence emission intensity decreases as the concentration of PdNPs increases. A PdNPs concentration-dependent fluorescence quenching phenomenon of FAM-labeled AFP aptamer is observed. As the AFP aptamer and PdNPs were both negatively charged, electrostatic attraction can be effectively excluded to be the reason for FRET occurrence. Thus it is ascribed to the strong coordination effect between AFP aptamer and PdNPs which brought FAM-labeled AFP aptamer in close to PdNPs and FRET occurres. The concentration of 0.21 mg·mL^{-1} for PdNPs was the optimum quenching effect to the FRET system. Therefore, we utilized a PdNPs concentration of 0.21 mg·mL^{-1} throughout the whole experiment.

The time dependence of fluorescence quenching efficiency indicates in Fig. 3c. From Fig. 3c, it only takes 38 mins to reach the quenching equilibrium. In the following fluorescence recovery experiments, 60 mins incubation time was chose for the fluorescence quenching experiment in order to ensure reaching the quenching equilibrium and obtain stable fluorescence signal.

Optimization of experimental conditions

In order to achieve the best sensing performance, a series of experimental conditions such as pH value of the system, the concentration of FAM-AFP aptamer, incubation time and incubation temperature were investigated. Respective data and Figures are given in the Electronic Supporting Material. The following experimental conditions were found to give best results: (a) optimal concentration of FAM-AFP aptamer: 180 nmol·L^{-1}; (b) optimal reaction temperature for AFP and AFP aptamer: 25 °C; (c) Best pH value: 6.5; (d) optimal reaction time for AFP and AFP aptamer: 70 mins.

Determination of AFP

Under the optimized experimental conditions, different concentrations of AFP were added to the FRET system to estimate the sensitivity. Figure 4a showed the fluorescence emission spectra of the FAM-AFP aptamer-PdNPs in the presence of different AFP concentrations from 0 to 1200 ng·mL^{-1}. The fluorescence intensity increases with increasing AFP concentration in the solution. The results are consistent with the proposed mechanism in Fig. 2, which indicates that the specific complexation of target protein (AFP) and its corresponding aptamer. The fluorescence recovery rate ($(F_1\text{-}F_0)/F_0$) is a AFP concentration-dependent manner, as indicated in Fig. 4b. Furthermore, a linear relationship between the fluorescence recovery rate of FAM and the concentration of AFP in the range of 5.0–150.0 ng·mL^{-1} is obtained (Fig. 4c). The regression equation is $Y = 0.33243 + 0.0127X$ with a correlation coefficient of 0.9923. The sensitivity, expressed as the slope of the calibration plot straight-line section, is calculated from the plot of Fig. 4c by means of linear regression. With the help of the linear regression, the sensitivity is calculated to be 0.0127 mL·ng^{-1}. The limits of detection (LOD), defined as $C_{LOD} = 3\sigma/K$, where σ is the standard deviation of blank measurements ($n = 5$), and K is the slope of calibration plot graph, has been calculated to be 1.38 ng·mL^{-1} at the signal-to-noise ratio of 3 [12].

The FRET aptamer nanoprobe is also compared with previously reported aptasensors targeting at AFP detection. As shown in Table 1, the electrochemical aptasensor methods yield very low detection limits. However, the whole experiment requires complicated electrode modifications, and its selectivity ability is poor. While the FRET aptamer nanoprobe demonstrates superiority in the detection speed and simplicity although its LOD is slightly higher than those of some previously reported aptasensors. The performance improvement of this FRET-based aptamer nanoprobe largely relies on the excellent fluorescence quenching ability of PdNPs towards FAM, with almost negligible non-specific fluorescence quenching.

Selectivity and specificity

To verify the selectivity and specificity of this FRET-based aptamer nanoprobe, some other proteins such as BSA, HAS, IgG, IgE and the mixture of BSA, HAS, IgG, IgE, AFP were added individually into the FAM-AFP aptamer-PdNPs FRET system in the place of AFP under the same experimental procedures and recorded the fluorescence intensity. As shown in Fig. 4d (column 1), the addition of AFP at a concentration of 100 ng·mL^{-1} led to a marked fluorescence increase; however, other protein at the same concentration of 100 ng·mL^{-1} (columns 3–6) does not result in a significant fluorescence increase. The result firmly demonstrates that this FRET-based aptamer nanoprobe exhibits excellent specificity towards

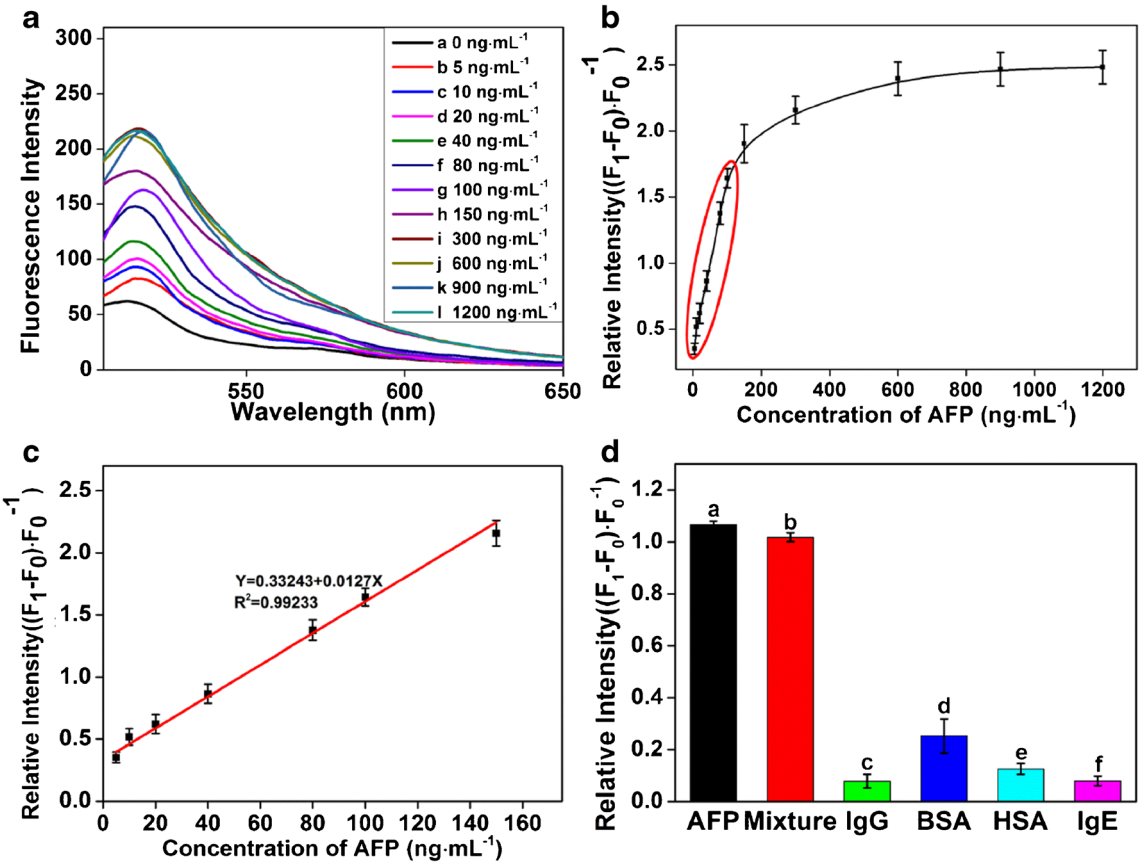

Fig. 4 **a** The fluorescence spectra of the FAM-aptamer/PdNPs in the presence of different AFP concentrations from 0 to 1200 ng·mL^{-1}; (**b**) The fluorescence recovery trend line in accordance with different concentration of AFP; (**c**) The linear relationship between the fluorescence recovery rate and the concentration of AFP within the range of 5.0–150.0 ng·mL^{-1}. (**d**) Relative fluorescence intensity of the fluorometric aptamer nanoprobe for AFP detection in the presence of different other proteins. The concentration of BSA, HAS, IgG, IgE were all 100 ng·mL^{-1} and the concentration of mixture of BSA, HAS, IgG, IgE, AFP was also 100 ng·mL^{-1}. Data were presented as average ± SD from three independent measurements. Experiments were conducted in HEPES buffer in the presence of 180 nmol·L^{-1} FAM-aptamer and 0.21 mg·mL^{-1} PdNPs under excitation at 480 nm and emission at 520 nm

AFP, in which the highly specific affinity between AFP aptamer and AFP took an important role. Furthermore, the mixture at the concentration of 100 ng·mL^{-1} (columns 2) has almost the same fluorescence increase with the same

Table 1 Comparison of the analytical parameters for a variety of aptasensor for AFP detection

Materials	Detection Method	Detection Range	LOD	References
AFP aptamer-coated magnetic beads	Chemiluminescence	50–800 ng·mL^{-1}	12.5 ng·mL^{-1}	[26]
Mixed self assembled aptamers and zwitterionic peptides	Electrochemical aptasensor	10.0 fg·mL^{-1} - 100.0 pg·mL^{-1}	3.1 fg·mL^{-1}	[27]
Thionin/reduced graphene oxide/gold nanoparticles	Electrochemical aptasensor	0.1–100.0 μg·mL^{-1}	50 ng·mL^{-1}	[24]
Graphene oxide	Electrochemical aptasensor	0.01–100 ng·mL^{-1}	3.0 pg·mL^{-1}	[21]
Concanavalin A- silver nanoparticles	Electrochemical aptasensor	50 pg·mL^{-1} - 10 ng·mL^{-1}	8.76 pg·mL^{-1}	[28]
dsDNA and methyl violet	Resonance light scattering aptasensor	5–100 ng·mL^{-1}	0.94 ng·mL^{-1}	[29]
Au NCs-MoS_2	Fluorescence aptasensor	0.5–60 ng·mL^{-1}	0.16 ng·mL^{-1}	[14]
Polyfluorene-based cationic conjugated polyelectrolytes	Fluorescence aptasensor	10–800 ng·mL^{-1}	1.76 ng·mL^{-1}	[25]
FAM-labeled AFP aptamer and PdNPs	Fluorescence aptasensor	5.0–150 ng·mL^{-1}	1.38 ng·mL^{-1}	This work

Table 2 Determination of AFP by the proposed aptasensor containing healthy human serum

AFP in human serum (ng/mL)	AFP Added (ng/mL)	Measured ($n = 3$) Average (ng/mL)	RSD(%)	Recovery (%)
0.06	20.0	22.6404	1.10	112.90
	40.0	39.3958	1.03	98.33
	60.0	64.8562	0.54	107.99

concentration of AFP (columns 1), which reveals that the FRET-based aptamer nanoprobe has good selectivity.

Practicability of the FRET-based aptamer nanoprobe

To evaluate the practicability of this assay, the FRET-based aptamer nanoprobe is used for determining the recoveries of three different concentrations of AFP by standard addition methods in human serum samples. As shown in Table 2, the recoveries and the relative standard deviation (RSD) varies from 98.33% to 112.90% and from 0.54% to 1.10% respectively. The results indicate that the FRET-based aptamer nanoprobe has great potential in practical application.

Conclusions

A highly sensitive FRET-based aptamer nanoprobe for AFP detection has been constructed based the excellent fluorescence quenching ability of PdNPs towards FAM. In the presence of AFP, the AFP aptamer forms a more compact and folded structure through the specific protein-aptamer interaction, which largely weakened the coordination effect between the AFP aptamer and PdNPs, resulting in an enhancement of fluorescence intensity of FAM. In the range of 5.0–150.0 ng·mL^{-1}, a linear relationship between the fluorescence recovery rate of FAM and the concentration of AFP was obtained with a readily achievable LOD of 1.38 ng·mL^{-1}. Moreover, this new method was successfully applied for sensitive detection of AFP in real human serum samples. We believe that the proposed strategy has great potential in the detection of other types of targets based on an appropriate aptamer.

Acknowledgements This work was supported by the National Nature Science Foundation of China (No. 81760534), the Foundation of Guangxi Key Laboratory of Automatic Detecting Technology and Instruments (No. YQ17114), and the Fund of the College students' innovative projects (Nos. 201710595110, 201810595006).

Compliance with ethical standards The author(s) declare that they have no competing interests.

References

1. Wang X, Wang Q (2018) Alpha-fetoprotein and hepatocellular carcinoma immunity. Can J Gastroenterol Hepatol 1:9049–9052
2. Xu T, Chi B, Wu F, Ma S, Zhan S, Yi M, Xu H, Mao C (2017) A sensitive label-free immunosensor for detection alpha-fetoprotein in whole blood based on anticoagulating magnetic nanoparticles. Biosens Bioelectron 95:87–93
3. Yuan Y, Li S, Xue Y, Liang J, Cui L, Li Q, Zhou S, Huang Y, Li G, Zhao Y (2017) A Fe_3O_4@au-basedpseudo-homogeneous electrochemical immunosensor for AFP measurement using AFP antibody-GNPs-HRP as detection probe. Anal Biochem 534:56–63
4. Xiang H, Wang Y, Wang M, Shao Y, Jiao Y, Zhu Y (2018) A redox cycling-amplified electrochemical immunosensor for alpha-fetoprotein sensitive detection via polydopamine nanolabels. Nanoscale 10:13572–13580
5. Uotila M, Ruoslahti E, Engvall E (1981) Two-site sandwich enzyme immunoassay with monoclonal antibodies to human alpha-fetoprotein. J Immunol Methods 42:11–15
6. Lu X, Mei T, Guo Q, Zhou W, Li X, Chen J, Zhou X, Sun N, Fang Z (2019) Improved performance of lateral flow immunoassays for alpha-fetoprotein and vanillin by using silica shell-stabilized gold nanoparticles. Mikrochim Acta 186:2–9
7. Li Y, Dong L, Wang X, Liu Y, Liu H, Xie M (2018) Development of graphite carbon nitride based fluorescent immune sensor for detection of alpha fetoprotein. Spectrochim Acta A Mol Biomol Spectrosc 196:103–109
8. Xu T, Chi B, Gao J, Chu M, Fan W, Yi M, Xu H, Mao C (2017) Novel electrochemical immune sensor based on Hep-PGA-PPy nanoparticles for detection of alpha-fetoprotein in whole blood. Anal Chim Acta 977:36–43
9. Li X, Guo Q, Cao W, Li Y, Du B, Wei Q (2014) Enhanced electrochemiluminescence from luminol at carboxyl graphene for detection of alpha-fetoprotein. Anal Biochem 457:59–64
10. Xu L, Gao Y, Kuang H, Liz-Marzan LM, Xu C (2018) MicroRNA-directed intracellular self-assembly of chiral nanorod dimers. Angew Chem Int Ed Engl 57:10544–10548
11. Zu F, Yan F, Bai Z, Xu J, Wang Y, Huang Y, Zhou X (2017) The quenching of the fluorescence of carbon dots: a review on mechanisms and applications. Mikrochim. Acta 184:1899–1914
12. Cheng X, Cen Y, Xu G, Wei F, Shi M, Xu X, Sohail M, Hu Q (2018) Aptamer based fluorometric determination of ATP by exploiting the FRET between carbon dots and graphene oxide. Mikrochim. Acta 185:144–151
13. Mohammadi S, Salimi A, Hamd-Ghadareh S, Fathi F, Soleimani F (2018) A FRET immunosensor for sensitive detection of CA 15-3 tumor marker in human serum sample and breast cancer cells using antibody functionalized luminescent carbon-dots and AuNPs-dendrimer aptamer as donor-acceptor pair. Anal Biochem 557:18–26
14. Xu S, Feng X, Gao T, Liu G, Mao Y, Lin J, Yu X, Luo X (2017) Aptamer induced multicoloured AuNCs-MoS_2 "switch on" fluorescence resonance energy transfer biosensor for dual color simultaneous detection of multiple tumor markers by single wavelength excitation. Anal Chim Acta 983:173–180
15. Gao R, Hao C, Xu L, Xu C, Kuang H (2018) Spiny nanorod and upconversion nanoparticle satellite assemblies for ultrasensitive detection of messenger RNA in living cells. Anal Chem 90:5414–5421
16. Raj M, Moon J-M, Goyal RN, Park D-S, Shim Y-B (2019) Simultaneous detection of ATP metabolites in human plasma and

urine based on palladium nanoparticle and poly(bromocresol green) composite sensor. Biosens Bioelectron 126:758–766
17. Xu L, Zhao S, Ma W, Wu X, Li S, Kuang H, Wang L, Xu C (2016) Multigaps embedded nanoassemblies enhance in situ Raman spectroscopy for intracellular telomerase activity sensing. Adv Funct Mater 26:1602–1608
18. Li H, Yang D, Li P, Zhang Q, Zhang W, Ding X, Mao J, Wu J (2017) Palladium nanoparticles-based fluorescence resonance energy transfer aptasensor for highly sensitive detection of aflatoxin M_1 in Milk. Toxins (Basel) 9:318–327
19. Li H, Shi L, Sun DE, Li P, Liu Z (2016) Fluorescence resonance energy transfer biosensor between upconverting nanoparticles and palladium nanoparticles for ultrasensitive CEA detection. Biosens Bioelectron 86:791–798
20. Ladju RB, Pascut D, Massi MN, Tiribelli C, Sukowati CHC (2018) Aptamer: a potential oligonucleotide nanomedicine in the diagnosis and treatment of hepatocellular carcinoma. Oncotarget 9:2951–2961
21. Yang S, Zhang F, Wang Z, Liang Q (2018) A graphene oxide-based label-free electrochemical aptasensor for the detection of alpha-fetoprotein. Biosens Bioelectron 112:186–192
22. Yang Q, Zhou L, Wu YX, Zhang K, Cao Y, Zhou Y, Wu D, Hu F, Gan N (2018) A two dimensional metal-organic framework nanosheets-based fluorescence resonance energy transfer aptasensor with circular strand-replacement DNA polymerization target-triggered amplification strategy for homogenous detection of antibiotics. Anal Chim Acta 1020:1–8
23. Dong L, Tan Q, Ye W, Liu D, Chen H, Hu H, Wen D, Liu Y, Cao Y, Kang J, Fan J, Guo W, Wu W (2015) Screening and identifying a novel ssDNA aptamer against alpha-fetoprotein using CE-SELEX. Sci Rep 5:15552–15561
24. Li G, Li S, Wang Z, Xue Y, Dong C, Zeng J, Huang Y, Liang J, Zhou Z (2018) Label-free electrochemical aptasensor for detection of alpha-fetoprotein based on AFP-aptamer and thionin/reduced graphene oxide/gold nanoparticles. Anal Biochem 547:37–44
25. Bao B, Su P, Zhu J, Chen J, Xu Y, Gu B, Liu Y, Wang L (2018) Rapid aptasensor capable of simply detect tumor markers based on conjugated polyelectrolytes. Talanta 190:204–209
26. Huang CJ, Lin HI, Shiesh SC, Lee GB (2012) An integrated microfluidic system for rapid screening of alpha-fetoprotein-specific aptamers. Biosens Bioelectron 35:50–55
27. Cui M, Wang Y, Jiao M, Jayachandran S, Wu Y, Fan X, Luo X (2017) Mixed self-assembled aptamer and newly designed zwitterionic peptide as antifouling biosensinginterface for electrochemical detection of alpha-fetoprotein. ACS Sens 2:490–494
28. Gao T, Zhi J, Mu C, Gu S, Xiao J, Yang J, Wang Z, Xiang Y (2018) One-step detection for two serological biomarker species to improve the diagnostic accuracy of hepatocellular carcinoma. Talanta 178:89–93
29. Chen F, Zhang F, Liu Y, Cai C (2018) Simply and sensitively simultaneous detection hepatocellular carcinoma markers AFP and miRNA-122 by a label-free resonance light scattering sensor. Talanta 186:473–480